# IKZF1 Deletions with COBL Breakpoints Are Not Driven by RAG-Mediated Recombination Events in Acute Lymphoblastic Leukemia

Bruno A. Lopes[*,†], Claus Meyer[†], Thayana C. Barbosa[*], Caroline P. Poubel[*], Marcela B. Mansur[*], Nicolas Duployez[‡], Matthew Bashton[§], Christine J. Harrison[§], Udo zur Stadt[¶], Martin Horstmann[¶,#], Maria S. Pombo-de-Oliveira[**], Chiara Palmi[††], Gianni Cazzaniga[††], Nicola C. Venn[‡‡], Rosemary Sutton[‡‡], Cristina N. Alonso[§§], Grigory Tsaur[¶¶], Sanjeev K. Gupta[##], Sameer Bakhshi[***], Rolf Marschalek[†] and Mariana Emerenciano[*]

[*]Molecular Cancer Study Group, Division of Clinical Research, Research Center, Instituto Nacional de Câncer, Rio de Janeiro, Brazil; [†]Diagnostic Center of Acute Leukemia, Institute of Pharmaceutical Biology, Goethe-University of Frankfurt, Frankfurt am Main, Germany; [‡]Laboratory of Hematology and Tumor Bank, Cancer Research Institute of Lille, CHRU of Lille, University Lille Nord de France, Lille, France; [§]Leukaemia Research Cytogenetics Group, Wolfson Childhood Cancer Research Centre, Northern Institute for Cancer Research, Newcastle University; [¶]Research Institute Children's Cancer Center, University Medical Center Hamburg-Eppendorf, Germany; [#]Clinic of Pediatric Hematology and Oncology, University Medical Center Hamburg-Eppendorf, Germany; [**]Pediatric Hematology-Oncology Program, Research Center, Instituto Nacional de Câncer, Rio de Janeiro, RJ, Brazil; [††]Centro Ricerca Tettamanti, Clinica Pediatrica, Dipartimento di Medicina e Chirurgia, Università degli Studi di Milano-Bicocca, Fondazione MBBM, Monza, Italy; [‡‡]Children's Cancer Institute, Lowy Cancer Research Centre UNSW, Sydney, New South Wales, Australia; [§§]Hematology and Oncology Department, Hospital de Pediatría Prof. Dr. Juan P. Garrahan, Buenos Aires, Argentina; [¶¶]Regional Children's Hospital No. 1, Yekaterinburg, Russia; Research Institute of Medical Cell Technologies, Yekaterinburg, Russia; [##]Laboratory Oncology Unit, Dr. BRA IRCH, All India Institute of Medical Sciences (AIIMS), New Delhi, India; [***]Dept. of Medical Oncology, Dr BRA IRCH, All India Institute of Medical Sciences (AIIMS), New Delhi, India

## Abstract

*IKZF1* deletion (ΔIKZF1) is an important predictor of relapse in both childhood and adult B-cell precursor acute lymphoblastic leukemia (B-ALL). Previously, we revealed that *COBL* is a hotspot for breakpoints in leukemia and could promote *IKZF1* deletions. Through an international collaboration, we provide a detailed genetic and clinical picture of B-ALL with *COBL* rearrangements (COBL-r). Patients with B-ALL and *IKZF1* deletion (*n* = 133) were included. *IKZF1* 1-8 were associated with large alterations within chromosome 7: monosomy 7 (18%),

isochromosome 7q (10%), 7p loss (19%), and interstitial deletions (53%). The latter included *COBL*-r, which were found in 12% of the *IKZF1* 1-8 cohort. Patients with *COBL*-r are mostly classified as intermediate cytogenetic risk and frequently harbor *ETV6*, *PAX5*, *CDKN2A/B* deletions. Overall, 56% of breakpoints were located within *COBL* intron 5. Cryptic recombination signal sequence motifs were broadly distributed within the sequence of *COBL*, and no enrichment for the breakpoint cluster region was found. In summary, a diverse spectrum of alterations characterizes Δ*IKZF1* and they also include deletion breakpoints within *COBL*. We confirmed that *COBL* is a hotspot associated with Δ*IKZF1*, but these rearrangements are not driven by RAG-mediated recombination.

## Introduction

B-cell precursor acute lymphoblastic leukemia (B-ALL) comprises multiple subtypes defined by structural and numerical chromosomal alterations. These initiating lesions include aneuploidy and chromosomal rearrangements, leading to expression of ectopic fusion proteins and/or to deregulation of gene expression. During the evolution of B-ALL, a series of secondary genomic alterations, such as DNA copy number alterations (CNAs) and sequence mutations, usually emerges [1]. These secondary events commonly involve deletions of genes that encode regulators of cell-cycle (*CDKN2A* and *CDKN2B*) and B-cell development (*PAX5* and *IKZF1*) [2].

*IKZF1* deletions occur in ~15% patients with B-ALL and are more recurrent in the *BCR-ABL1* and Philadelphia-like subgroups, affecting more than 70% and 40% of the patients, respectively [3]. *IKZF1* is located within chromosome band 7p12 and codifies the transcription factor IKAROS. It has two main domains: a DNA-binding zinc finger domain (encoded by exons 4-6) and a zinc finger dimerization domain (encoded by exon 8). Some intragenic *IKZF1* deletions impair its DNA-binding domain resulting in a dominant-negative effect (e.g. Δ4-7), while deletions of the whole gene (Δ1-8), as well as deletions of exons 1-2 (e.g. Δ2-3) lead to the gene haploinsufficiency. *IKZF1* deletions have been associated with dismal prognosis in both pediatric and adult B-ALL [4,5], despite the type of deletion [6]. Interestingly, sequencing of *IKZF1* breakpoints suggested that aberrant recombination activating gene (RAG)–mediated recombination is responsible for these deletions [7]. Due to their clinical relevance, the identification of *IKZF1* deletions has become an essential prognostic biomarker over the last decade. Hence, aiming to detect these deletions, we developed a rapid and efficient polymerase chain reaction (PCR)–based method [8]. Recently, by delineating the genetic landscape of *IKZF1* Δ1-8, we identified *COBL* (*COBL cordon-bleu WH2 repeat protein*) gene as an originating hotspot for *IKZF1* deletions [9]. Here we established an international collaboration to enable a detailed genetic and clinical characterization of B-ALL with *COBL* rearrangements (*COBL*-r).

## Material and Methods

### Patients

This study included 146 patients diagnosed with B-ALL and *IKZF1* deletions. This patient cohort comprised two independent groups. The first one included 133 patients with 1) *IKZF1* complete deletion, Δ1-8 (*n* = 104); or 2) intragenic deletion of *IKZF1* including exon 8, Δn-8 (*n* = 29). The second group referred to 13 patients already diagnosed with *IKZF1* deletions and *COBL*-r at collaborating centers [8–10].

Patient samples and information were obtained through the cooperative efforts of nine centers worldwide, and the project was conducted in accordance with the declaration of Helsinki.

### Detection of IKZF1 Deletions and CNAs

*IKZF1* deletions and CNAs in *EBF1*, *JAK2*, *CDKN2A*, *CDKN2B*, *PAX5*, *ETV6*, *BTG1*, *RB1*, and the pseudoautosomal region 1-PAR1 (*SHOX*, *CRLF2*, *C2F2RA*, *IL3RA*, and *P2RY8*) were determined by either multiplex ligation-dependent probe amplification (MLPA), or single nucleotide polymorphism (SNP) array analyses. The SALSA MLPA P335-(A3-B2) and/or SALSA MLPA P202-B1 (MRC Holland) were used for MLPA experiments, and the data analyses were performed using Coffalyser software. The CytoScan HD Array (Affymetrix) assessed the occurrence of CNAs in the Brazilian (partially), British, and French cohorts. Data were analyzed with Chromosome Analysis Suite software, version 3.2 (Applied Biosystems), and the GRCh38/hg38 build of the Human Genome Assembly.

### Characterization of COBL Breakpoints

We developed customized MLPA assays for the screening of CNAs within chromosome 7. The probes' design and assay conditions have been previously described [9]. To validate our SNP array and MLPA findings, we performed either multiplexed long-distance PCR (M-PCR) or long-distance inverse (LDI)-PCR. These PCR approaches allowed us to confirm *COBL*-r and to determinate the breakpoints at nucleotide level.

### Patient Data and Survival Analyses

For the comparison of laboratory and clinical data between patients with or without *COBL*-r, we used the Pearson $\chi^2$ test. Overall survival (OS) was defined as the time in months from the date of diagnosis to death or to the last follow-up assessment for patients alive. Kaplan-Meier method was used to estimate OS rates of patients according to *COBL* status with differences compared by the log-rank test. Statistical analyses were performed using R software, version 3.5.2, and *P* values < .05 were considered statistically significant.

### Analysis of Activation-Induced Deaminase (AID) or RAG Recognition Signal Sequences in Recombined COBL Alleles

An agnostic search for motifs located within fragments spanning 50 bp from the breakpoint junctions of *COBL*-r was performed using MEME. The limit of output motifs was set to 5, and width ranged from 2 to 15 bp. The FIMO (Find Individual Motif Occurrences) tool was used for the analysis of WGCW and CG sequences, and the recombination signal sequence (RSS) consensus sequence was used to search for cryptic RSS sequences [11,12].
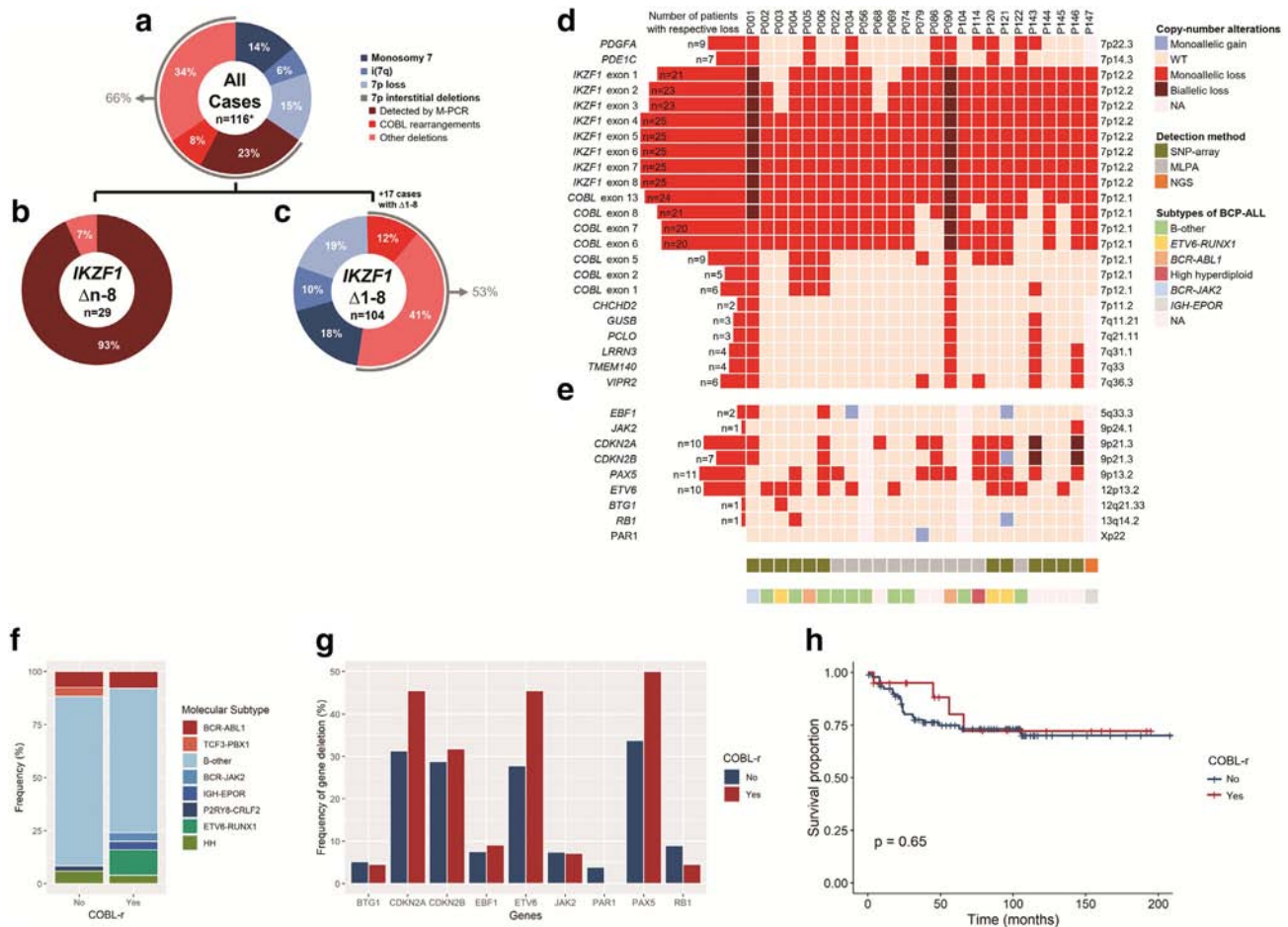
**Figure 1.** Genetic alterations associated with *IKZF1* deletions in B-ALL. (A) Patients with *IKZF1* deletions spanning its exon 8 presented four types of aberrations on chromosome 7: monosomy 7; isochromosome 7q, i(7q); 7p loss; and interstitial deletions within 7p arm. *One cohort of 17 cases comprising only complete deletions of *IKZF1* was excluded from this analysis because they would lead to a biased estimative of CNAs' frequencies among patients with *IKZF1* deletions overall. Then, patients were divided into two groups: (B) intragenic deletions of *IKZF1* spanning its exon 8 ($n = 29$) and (C) complete deletions of *IKZF1* ($n = 104$). (D) The *COBL* rearrangements were identified in 25 patients. Most of the deletions spanned between *IKZF1* exon 1 and *COBL* intron 5, although they presented variable size. (E) These patients had additional alterations, such as *ETV6*, *PAX5*, *CDKN2A*, and *CDKN2B* deletions. *NA*, not available. (F) Distribution of molecular subtypes of B-ALL among patients with or without *COBL*-r. Legend colors illustrate alterations associated with high risk (red), intermediate risk (blue), and good risk (green). *HH*, high hyperdiploidy. (G) The frequency of deletions in genes associated with B-ALL was compared according to *COBL* status. *PAX5*, *CDKN2A*, *CDKN2B*, and *ETV6* deletions were recurrently observed; however, the frequency of these CNAs was similar for all these genes, as indicated by *P* values above each bar. *PAR1*, pseudoautosomal region 1. (H) No significant difference was observed when comparing the overall survival of B-ALL patients with *COBL*-r vs. *COBL* wild type ($P = .65$).

## Results

Most of the deletions encompassing *IKZF1* exon 8 were classified as whole-gene deletions (Δ1-8: 78% vs. Δn-8: 22%). The CNAs found in the cohort were associated with monosomy 7 (14%; $n = 16$); isochromosome 7q (6%; $n = 7$): 7p loss (15%; $n = 17$), and interstitial deletions within 7p (66%; $n = 76$) (Figure 1A). Among the Δn-8 group, most of the alterations (93%) were *IKZF1* deletions detectable by the M-PCR, i.e., Δ2-8 or Δ4-8 (Figure 1B). Alternatively, 47% of the Δ1-8 group presented with aberrations involving loss of the whole 7p, such as monosomy 7 (18%; $n = 19$), isochromosome 7q (10%; $n = 10$), and 7p loss (19%; $n = 20$). The remaining 55 patients (53%) harbored interstitial deletions; *COBL*-r were found in 12% of the Δ1-8 cohort (Figure 1C).

We identified *COBL*-r in 25 B-ALL cases with *IKZF1* deletions (Figure 1D). *COBL*-r were detected by MLPA screening in 133 patients with B-ALL and *IKZF1* deletions ($n = 12$) or SNP array/ NGS investigation performed at collaborating centers ($n = 13$), as

described in the methodology. The loss of genes located within 9p locus — *PAX5* ($n = 11$), *CDKN2A* ($n = 10$), and *CDKN2B* ($n = 7$) — and *ETV6* deletions ($n = 10$) were the most recurrent additional alterations among these patients (Figure 1E). Demographic and laboratory data for the 25 patients with *COBL*-r showed they included 17 males and 8 females who were mainly children and adolescents ($n = 21$), with a median age at diagnosis of 5.5 years (range 1-59 years) and a median white blood cell count of $7.5 \times 10^9$/l (range $1.5$-$459.6 \times 10^9$/l) (Table 1). The patients were treated on diverse therapy protocols (Table 2). Seven patients relapsed within a median of 5.5 years (range 1.4-16.3 years), and six of them experienced isolated disease recurrence in the bone marrow ($n = 5$) or testes ($n = 1$). One patient relapsed at both sites: bone marrow and central nervous system. The median follow-up was 5.1 years (range 0.3-16.3 years), and the five deaths (mainly in patients with early relapse) occurred at a median 4.2 years (range 0.3-5.5 years) following diagnosis. In addition, the comparison between patients

**Table 1.** Demographic and Laboratory Characteristics of B-ALL Cases with *COBL* Rearrangements.[*]

| Patient | Age (Years) | Gender | WBC (×10⁹/l) | Blasts at BM | 5′ Breakpoint | 3′ Breakpoint | Detection Method | Karyotype |
|---|---|---|---|---|---|---|---|---|
| P004 | 1 | F | 96.000 | 95% | *ELMO1* intron 14 | Upstream *COBL* | SNP array | 46,XX,+2,t(3;16)(p21;p13),del(4)(q22),−7, der(12)t(7;12)(q11;p13),−13,+16,−18,−19,+mar1,+mar2 |
| P034 | 1 | M | 3.400 | 98% | *RAD50* intron 5 | *COBL* intron 5 | LDI-PCR | NA |
| P086 | 1 | M | 5.000 | 95% | 7pter | *COBL* intron 7 | MLPA/LDI-PCR | NA |
| P120 | 1 | F | 459.600 | 80% | 7p14 | *COBL* intron 5 | SNP array/M-PCR | NA |
| P056 | 2 | F | 1.600 | 98% | *SPATA* intron 1 | *COBL* intron 5 | LDI-PCR | 46,XX |
| P122 | 2 | M | 13.400 | 40% | 7pter | *COBL* intron 7 | MLPA | NA |
| P145 | 2 | F | 92.000 | 98% | *TCRGC2* intron 1 | *COBL* intron 13 | SNP array | 47,XX,del(7)(p11),+10,add(12)(p13),del(12)(p11.2)[4] |
| P022 | 4 | F | 7.500 | 85% | 7p12 | *COBL* intron 2-5 | MLPA | 46,XX |
| P003 | 5 | M | 10.000 | 95% | *IKZF1* intron 3 | *COBL* intron 5 | SNP array/M-PCR | 46,XY |
| P074 | 5 | M | 16.400 | 78% | 7p12.1 | *COBL* intron 5 [‡] | LDI-PCR | NA |
| P079 | 5 | F | 5.700 | 88% | 7p | *COBL* intron 8-13 | MLPA | NA |
| P121 | 5 | F | 7.470 | 50% | 7p12.2 | *COBL* intron 5 | SNP array/M-PCR | NA |
| P144 | 5 | M | 31.000 | NA | 7p14.2 | *COBL* intron 5 | SNP array | 47,XY,+X,del(16)(q13),i(17)(q10), ider(21)(q10)dup(21)(q?)[3]/ 47,idem,add(7)(p1)[3] |
| P002 | 6 | M | 115.000 | 97% | 7p12.2 | *COBL* intron 5 | SNP array/M-PCR | 46,XY,del(6)(q21q25),der(12)del(12) (p11p13)t(12;17)(p13;q11),der(17)t(12;17) |
| P069 | 10 | F | 204.000 | 89% | *IKZF1* intron 1 | *COBL* intron 5 | LDI-PCR | NA |
| P146 | 11 | M | 1.500 | 90% | *SPATA* intron 2 | *COBL* intron 5 | SNP array | 48,XY,+X,?t(6;20)(p1;q1),?t(7;9)(p1;p2), i(9)(q10),+12,der(21)dup(21)(q?)[9] |
| P068 | 12 | M | NA | NA | *IKZF1* intron 3 | *COBL* intron 5 | RNA-seq/LDI-PCR | 48,XY,+X,del(4)(q25),−7,del(9)del(9) t(4;9)(q25;p13),+21,+mar[cp8]/ |
| P104 | 13 | M | 1.680 | 84% | 7p14 | *COBL* intron 5 | MLPA | 46,XY,del(7)(p14),der(9;12)(q10;q10),+mar[6] |
| P090 | 15 | M | 4.500 | 83% | 7p22 | *COBL* intron 5 | MLPA | NA |
| P114 | 16 | M | 55.000 | 45% | 7p | *COBL* intron 2-5 | MLPA | NA |
| P143 | 16 | M | 6.200 | 96% | *COBL* intron 1 [†] | 7p12.1 | SNP array | 46,XY,idic(9)(p13)[1]/ 45,idem,−7[3]/ 45,idem,add(2)(p25),−7[9] |
| P147 | Adolescent | M | NA | NA | *SUN3* intron 5 | *COBL* intron 5 | NGS | NA |
| P005 | 21 | M | 2.820 | 90% | 7pter | Upstream *COBL* | SNP array | 46,XY,t(9;22)(q34;q11) |
| P006 | 38 | M | 3.040 | 67% | *VWC2* intron 3 | Upstream *COBL* | SNP array | 46,XY |
| P001 | 59 | M | 58.000 | 75% | 7p12 | *COBL* intron 7 [§] | SNP array | 45,XY,−7,t(9;22;15)(p24;q11;q21),add(9)(p13) |

*BM*, bone marrow; *LDI-PCR*, long-distance inverse PCR; *M-PCR*, multiplex PCR; *MLPA*, multiplex ligation-dependent probe amplification; *NA*, not available; *WBC*, white blood cell count.
[*] In this case, blast percent was estimated from peripheral blood.
[†] Patient had *COBL* rearrangement and 7p12.3::*GRB10* intron 5 deletion.
[‡] Patient had an inversion within *COBL* intron 5.
[§] Patient had *COBL* rearrangement and monosomy 7.

**Table 2.** Clinical Characteristics and Outcome of B-ALL Cases with *COBL* Rearrangements

| Patient | Clinical Trial | CNS Disease | MRD Day 33 | MRD Day 78 | PR | CMR Day 33 | Relapse | Outcome | Follow-Up (Months) |
|---|---|---|---|---|---|---|---|---|---|
| P147 | AALL0232_1 | NA | NA | NA | NA | NA | NA | NA | NA |
| P068 | AALL0331/UKALLR3 | No | Negative | Negative | NA | Yes | BM | Dead | 45 |
| P034 | AIEOP-BFM ALL2000 | No | Negative | Negative | Good | Yes | No | 1st CR | 96 |
| P022 | AIEOP-BFM ALL2000 | No | Negative | Negative | Good | Yes | No | 1st CR | 79 |
| P114 | AIEOP-BFM ALL2000 | No | NA | NA | Good | Yes | NA | Dead | NA |
| P120 | AIEOP-BFM ALL2000 | No | Positive | Positive | Poor | No | No | Dead | 4 |
| P104 | ALL IC 2009 | Yes | Negative | Negative | Good | Yes | No | 1st CR | 38 |
| P145 | UKALL2003 | No | Negative | Negative | NA | Yes | No | 1st CR | 105 |
| P146 | UKALL2003 | No | Negative | NA | NA | Yes | BM, CNS | Dead | 66 |
| P144 | UKALL97 | No | NA | NA | NA | Yes | No | 1st CR | 26 |
| P143 | UKALL97 | No | NA | NA | NA | Yes | No | 1st CR | 167 |
| P003 | CAALLF01 | No | Negative | NA | Good | Yes | NA | 1st CR | 4 |
| P079 | COALL 05-92 | No | NA | NA | NA | Yes | No | 1st CR | 161 |
| P086 | COALL 06-97 | No | Negative | NA | NA | Yes | Testes | 2nd CR | 195 |
| P074 | COALL 06-97 | No | Negative | NA | NA | Yes | BM | 2nd CR | 154 |
| P069 | COALL 07-03 | No | Positive | NA | NA | No | No | 1st CR | 123 |
| P004 | EORTC 58081 | No | Negative | Negative | Good | Yes | No | 1st CR | 49 |
| P090 | EsPhALL | No | Positive | NA | Good | Yes | Isolated BM | Dead | 56 |
| P006 | FRALLE 93 | No | Positive | Positive | Poor | Yes | Yes | Relapse | 192 |
| P002 | FRALLE BT | No | Positive | Negative | Poor | Yes | No | 1st CR | 15 |
| P122 | GBTLIALL99 | No | NA | NA | Good | Yes | NA | Alive | NA |
| P121 | GBTLIALL99 | No | Negative | Negative | Good | Yes | No | Alive | NA |
| P005 | GRAAPH | No | Positive | Positive | Not evaluable | Yes | No | 1st CR | 27 |
| P056 | NA | No | Positive | NA | Good | Yes | BM | Lost follow-up | 17 |
| P001 | NA | No | Positive | NA | Good | Yes | No | SCT; alive | 9 |

*BM*, bone marrow; *CNS*, central nervous system; *CMR*, complete morphological remission; *MRD*, minimal residual disease; *NA*, not available; *PR*, prednisone response; *SCT*, stem-cell transplantation; *WBC*, white blood cell count. MRD-negative status was defined as <0.01% leukemic cells in bone marrow and peripheral blood.

with *COBL*-r vs. *COBL* wild-type revealed that both groups presented similar laboratory and clinical characteristics (Table 3). Among the B-ALL cytogenetic abnormalities, *TCF3-PBX1* and *ETV6-RUNX1* were exclusively found in patients without or with *COBL*-r, respectively (Figure 1*F*). Although we did not observe any significant difference in the frequency of additional gene deletions when comparing patients with vs. without *COBL*-r, it is worthy of note that *CDKN2A*, *ETV6*, and *PAX5* deletions were more frequent in patients with *COBL*-r (Figure 1*G*). Follow-up data were available for 111 B-ALL patients with (*n* = 20) or without *COBL*-r (*n* = 91). The OS of patients with *COBL*-r was similar to those with *IKZF1* deletion only (hazard ratio, 1.278; 95% CI, 0.35-4.68; *P* = .646) (Figure 1*H*).

The breakpoints of the *COBL*-r were determined at nucleotide level in 11 of the 25 cases, and 56% of breakpoints were located within *COBL* intron 5 (Figure 2*B*). To address the possible causes of these breakpoints, we first performed an agnostic motif search. This analysis identified the motif CASWGTGG (E-value = 0.87) within all 22 breakpoint sequences of *COBL*-r (Figure 2*A*; Supplementary Table S1). CASWGTG is similar to the heptamer of the RAG RSS, which is composed of a heptamer (5′-CACAGTG-3′) and a nonamer (5′-ACAAAAACC-3′) sequence, interspaced by 12 or 23 random nucleotides associated to RAG-type rearrangements. Since the nonamer was absent in our first analysis, we then investigated the presence of complete motifs associated with the occurrence of rearrangements in leukemia: cryptic RSS sequence (RAG-type fusions), WGCW (AID-type fusions), and CG sequences. WGCW and CG sequences were not found; however, we identified cryptic RSS in 5 out of 22 breakpoint regions, although none of them were spanning breakpoints within *COBL* (Supplementary Table S2).

**Table 3.** Demographic and Laboratory Data of Patients with B-ALL[*]

| | *COBL* Rearrangement | | *P* Value |
|---|---|---|---|
| | No *n* = 121 | Yes *n* = 25 | |
| | *n* (%) | *n* (%) | |
| Gender | | | 0.473 |
| Male | 48 (39.7) | 8 (32.0) | |
| Female | 73 (60.3) | 17 (68.0) | |
| Age at diagnosis | | | 0.701 |
| <1 year | 2 (1.7) | 0 (0.0) | |
| 1-9 years | 49 (41.5) | 12 (48.0) | |
| ≥10 years | 67 (56.8) | 13 (52.0) | |
| WBC (×10⁹/L) | | | 0.948 |
| <50 | 85 (70.2) | 16 (69.6) | |
| ≥50 | 36 (29.8) | 7 (30.4) | |
| NCI risk | | | 0.797 |
| Standard | 69 (58.0) | 14 (60.9) | |
| High | 50 (42.0) | 9 (39.1) | |
| CNS disease | | | 0.741 |
| No | 96 (94.1) | 23 (95.8) | |
| Yes | 6 (5.9) | 1 (4.2) | |
| Prednisone response | | | 0.143 |
| Good | 66 (91.7) | 11 (78.6) | |
| Poor | 6 (8.3) | 3 (21.4) | |
| Relapse | | | 0.607 |
| No | 75 (70.8) | 13 (65.0) | |
| Yes | 31 (29.2) | 7 (35.0) | |
| Outcome | | | 0.604 |
| Alive | 94 (77.7) | 20 (83.3) | |
| Dead | 27 (22.3) | 4 (16.7) | |

*WBC*, white blood cell count; *NCI*, National Cancer Institute of US; *CNS*, central nervous system.
[*] Pearson χ² calculation.

Additionally, we performed a robust analysis for the identification of cryptic RSSs within the whole sequence of *COBL* (Figure 2, C-D). The results revealed a broad distribution of this motif throughout the gene and no enrichment for the breakpoint cluster located in intron 5 of *COBL*.

## Discussion

In this study, among the Δn-8 group, the majority of the alterations were *IKZF1* deletions which had already been detected by the M-PCR method [8]. Since the remaining Δn-8 samples harbored deletions restricted to *IKZF1*, either they had DNA fusions outside the breakpoint cluster region of *IKZF1* or M-PCR failed to detect them. Among the Δ1-8 group, *COBL*-r were found in 12% of the patients. This result revealed that *COBL*-r are more frequent among Δ1-8 but rarely related to Δn-8. Although *COBL*-r were not detected within the Δn-8 group for the cases included in the current proposal, we found these deletions in patients with *COBL*-r from a previous study [9]. These patients had *IKZF1-COBL* fusions, which involved *IKZF1* intron 1 (*n* = 1) or intron 3 (*n* = 2) and *COBL* intron 5.

Confirming the idea that *COBL* represents a genomic hotspot for *IKZF1* deletions in B-ALL [9], we identified *COBL*-r in 25 B-ALL cases with *IKZF1* deletions. Although either good (*ETV6-RUNX1*, high hyperdiploid) or high-risk (*BCR-ABL1*) cytogenetic groups have been observed in some of these patients, most of them had the so-called "B-other" subclassification with either normal or other abnormal (*BCR-JAK2*, *IGH-EPOR*) cytogenetic profile. In the current genetic risk stratification, many cases with *COBL*-r would then be classified as intermediate cytogenetic risk. We found that these patients also presented other secondary abnormalities commonly identified in B-ALL, such as *PAX5* and *CDKN2A/B* and *ETV6* deletions. This combination is of special interest because these patients could benefit from the newly proposed combined risk stratification strategies, such as *IKZF1*^plus or the UKALL-CNA classifiers [13–15]. Considering that patients with B-ALL share similar laboratory and clinical characteristics regardless of *COBL* involvement, *IKZF1* deletions may play a major role on risk stratification for these patients.

Regarding the breakpoints of the *COBL*-r, it is remarkable that 56% of them were located within *COBL* intron 5, although this region represents only 16% (47,770 out of 300,587 bp) of the entire gene. Based on this observation, we formulated two hypotheses to explain the presence of a hotspot for breakpoints within *COBL*: 1) the production of a truncated COBL protein, encoded by exons 1-5 only, could have a role on leukemogenesis, or 2) there is a breakage mechanism involving *COBL* intron 5, thus enriching this area for gene rearrangements.
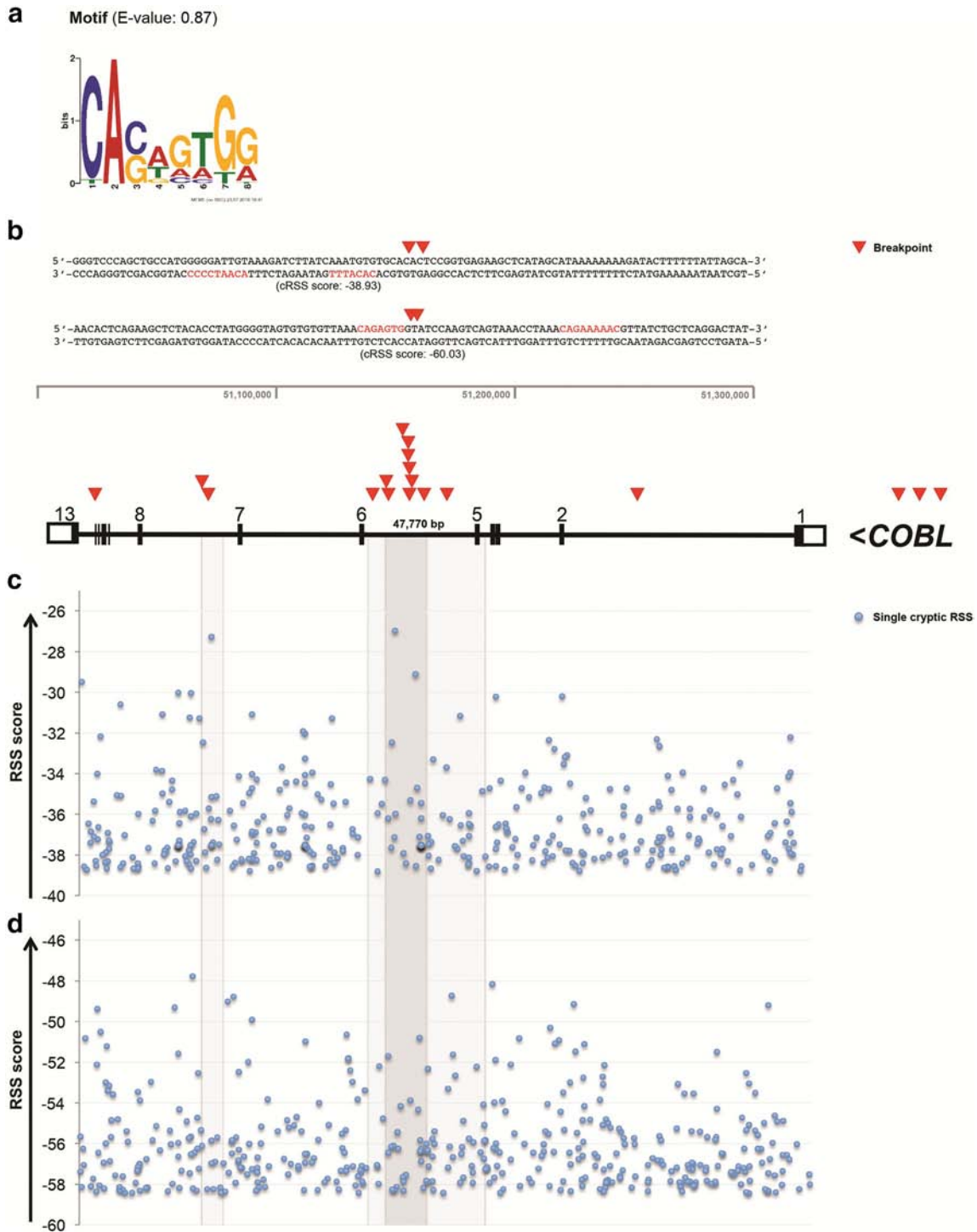
COBL protein has three Wiskott-Aldrich syndrome protein homology 2 domains for actin binding. It shows substantial expression in neurons and muscle cells, although levels are low in blood [16]. COBL functions as an actin nucleator, controlling neuronal morphology and development [17]. Considering that COBL does not play a direct role in lymphoid development, the enrichment of *COBL*-r in B-ALL is more likely to be related to mechanisms controlling DNA breakage and promotion of genetic fusions.

Usually, genetic rearrangements in lymphoid malignancies are caused by either AID or the RAG complex. Therefore, we searched for motifs located within the breakpoint junctions of *COBL*-r, which could potentially provide a rational explanation for the observed

**Figure 2.** Identification of motifs within the breakpoint sequences. (A) An agnostic motif search using MEME identified the sequence CASWGTGG (E-value = 0.87) among 22 breakpoint sequences. (B) The map of 19 deletion breakpoints (red triangles) within *COBL* revealed a hotspot located at intron 5. Three breakpoints were detected within a downstream region of 7p12.1. The sequences highlight two breakpoint clusters located at *COBL* intron 5. The mapped cryptic recombination signal sequences were not statistically significant. The cryptic recombination signal sequences (cRSS) with a spacer of 12-bp (c) and 23-bp (d) were mapped along *COBL* gene. The highest RIC scores represent cRSS (blue dots) associated with RSS functionality. The gray area highlights the *COBL* intron 5 and breakpoint cluster regions.

chromosomal rearrangements. RSSs are recognized by RAG enzymes during V(D)J recombination, and previous studies have located cryptic RSS immediately internal to the breakpoints of intragenic deletions of *IKZF1*[7]. Although the mutual motif within sequences spanning the breakpoints was similar to the heptamer sequence, our results do not support the idea that aberrant RAG-mediated recombination is the mechanism responsible for *IKZF1* and *COBL* codeletions.

In summary, our results highlight *COBL* as a hotspot for interstitial deletions within chromosome 7, especially for deletions including the *IKZF1* gene. Most of the *COBL*-r arose within *COBL* intron 5, leading to complete deletion of *IKZF1*; nevertheless, we also observed fusions between both genes. The analysis of the breakpoint sequences revealed a common motif resembling the heptamer of recombination signal sequence, but the analysis of the whole consensus sequence did not provide evidence for RAG-mediated recombination. Lastly, our study demonstrates that patients with *IKZF1* deletions are associated with worse outcome regardless of *COBL*-r.

Supplementary data to this article can be found online at https://doi.org/10.1016/j.tranon.2019.02.002.

## Conflict of Interest

The authors declare no conflict of interest.

## Author Contribution

Conception and design: B. A. L., C. M., R. M., M. E. Experiments, data analysis, and interpretation: B. A. L., C. M., T. C. B., C. P. P., N. D., M. B., U. S., C. P., N. C. V., R. M., M. E. Provision of samples, data collection, and assembly: B. A. L., M. B. M., N. D., C. J.H., U. S., M. H., M. S. P. O., G. C., R. S., C. N. A., G. T., S. G., S. B. Writing and/or revision of the manuscript: B. A. L., R. M., M. B. M., C. J. H., G. C., R. S., C. N. A., M. E. Final manuscript approval: all authors.

## References

[1] Greaves M (2018). A causal mechanism for childhood acute lymphoblastic leukaemia. *Nat Rev Cancer* **18**, 471–484.

[2] Barbosa TC, Terra-Granado E, Quezado Magalhaes IM, Neves GR, Gadelha A, Guedes Filho GE, Souza MS, Melaragno R, Emerenciano M, and Pombo-de-Oliveira MS (2015). Frequency of copy number abnormalities in common genes associated with B-cell precursor acute lymphoblastic leukemia cytogenetic subtypes in Brazilian children. *Cancer Genet* **208**, 492–501.

[3] Mullighan CG, Goorha S, Radtke I, Miller CB, Coustan-Smith E, Dalton JD, Girtman K, Mathew S, Ma J, and Pounds SB, et al (2007). Genome-wide analysis of genetic alterations in acute lymphoblastic leukaemia. *Nature* **446**, 758–764.

[4] Dorge P, Meissner B, Zimmermann M, Moricke A, Schrauder A, Bouquin JP, Schewe D, Harbott J, Teigler-Schlegel A, and Ratei R, et al (2013). IKZF1 deletion is an independent predictor of outcome in pediatric acute lymphoblastic leukemia treated according to the ALL-BFM 2000 protocol. *Haematologica* **98**, 428–432.

[5] Mullighan CG, Su X, Zhang J, Radtke I, Phillips LA, Miller CB, Ma J, Liu W, Cheng C, and Schulman BA, et al (2009). Deletion of IKZF1 and prognosis in acute lymphoblastic leukemia. *N Engl J Med* **360**, 470–480.

[6] Boer JM, van der Veer A, Rizopoulos D, Fiocco M, Sonneveld E, de Groot-Kruseman HA, Kuiper RP, Hoogerbrugge P, Horstmann M, and Zaliova M, et al (2016). Prognostic value of rare IKZF1 deletion in childhood B-cell precursor acute lymphoblastic leukemia: an international collaborative study. *Leukemia* **30**, 32–38.

[7] Mullighan CG, Miller CB, Radtke I, Phillips LA, Dalton J, Ma J, White D, Hughes TP, Le Beau MM, and Pui CH, et al (2008). BCR-ABL1 lymphoblastic leukaemia is characterized by the deletion of Ikaros. *Nature* **453**, 110–114.

[8] Meyer C, Zur Stadt U, Escherich G, Hofmann J, Binato R, Barbosa TC, Emerenciano M, Pombo-de-Oliveira MS, Horstmann M, and Marschalek R (2013). Refinement of IKZF1 recombination hotspots in pediatric BCP-ALL patients. *Am J Blood Res* **3**, 165–173.

[9] Lopes BA, Meyer C, Barbosa TC, Zur Stadt U, Horstmann M, Venn NC, Heatley S, White DL, Sutton R, and Pombo-de-Oliveira MS, et al (2016). COBL is a novel hotspot for IKZF1 deletions in childhood acute lymphoblastic leukemia. *Oncotarget* **7**, 53064–53073.

[10] Duployez N, Nibourel O, Ducourneau B, Grardel N, Boyer T, Bories C, Darre S, Coiteux V, Berthon C, and Preudhomme C, et al (2016). Acquisition of genomic events leading to lymphoblastic transformation in a rare case of myeloproliferative neoplasm with BCR-JAK2 fusion transcript. *Eur J Haematol* **97**, 399–402.

[11] Bailey TL, Johnson J, Grant CE, and Noble WS (2015). The MEME suite. *Nucleic Acids Res* **43**, W39–W49.

[12] Grant CE, Bailey TL, and Noble WS (2011). FIMO: scanning for occurrences of a given motif. *Bioinformatics* **27**, 1017–1018.

[13] Hamadeh L, Enshaei A, Schwab C, Alonso CN, Attarbaschi A, Barbany G, den Boer ML, Boer JM, Braun M, and Dalla Pozza L, et al (2019). Validation of the United Kingdom copy-number alteration classifier in 3239 children with B-cell precursor ALL. *Blood Adv* **3**, 148–157.

[14] Moorman AV, Enshaei A, Schwab C, Wade R, Chilton L, Elliott A, Richardson S, Hancock J, Kinsey SE, and Mitchell CD, et al (2014). A novel integrated cytogenetic and genomic classification refines risk stratification in pediatric acute lymphoblastic leukemia. *Blood* **124**, 1434–1444.

[15] Stanulla M, Dagdan E, Zaliova M, Moricke A, Palmi C, Cazzaniga G, Eckert C, Te Kronnie G, Bourquin JP, and Bornhauser B, et al (2018). IKZF1(plus) defines a new minimal residual disease-dependent very-poor prognostic profile in pediatric B-cell precursor acute lymphoblastic leukemia. *J Clin Oncol* **36**, 1240–1249.

[16] G.T. Consortium (2013). The Genotype-Tissue Expression (GTEx) project. *Nat Genet* **45**, 580–585.

[17] Ahuja R, Pinyol R, Reichenbach N, Custer L, Klingensmith J, Kessels MM, and Qualmann B (2007). Cordon-bleu is an actin nucleation factor and controls neuronal morphology. *Cell* **131**, 337–350.